CrossMark

AFSTi
Empowering food professionals

ORIGINAL ARTICLE

Characterization of molecular structures of theaflavins and the interactions with bovine serum albumin

Shicheng Lei[1] · Donglan Xu[1] · Muhammad Saeeduddin[1] · Asad Riaz[1] ·
Xiaoxiong Zeng[1]

Abstract In this study, theaflavins (TF1, TF2A, TF2B and TF3) were prepared from black tea and their interaction with bovine serum albumin (BSA) was explored by fluorescence and CD spectroscopy. The results showed that the structures of theaflavins exhibited significant effects on the binding/quenching process, and the binding affinity increased with the increase of molecular weight of theaflavins and the presence of galloyl moiety. The quenching effects showed a sequence as TF3 > TF2A > TF2B > TF1, demonstrating the important role of the galloyl moiety on the C-3 position of theaflavins. CD spectra indicated that TF3 in high concentration could change the skeleton structure of BSA and induce the unfolding of BSA secondary structure. The present results provide a new perspective for better understanding of the likely physiological fate of theaflavins and help to control the functional characteristics of food.

Keywords Theaflavins · EGCG · Bovine serum albumin · Interaction · Fluorescence quenching

Introduction

Tea, made from the fresh leaves and buds of tea plant (*Camellia sinensis*), is one of the most widely consumed beverages in the world. Depending on the manufacturing process, tea beverages are classified into three major types, such as green tea (non-fermented), black tea (full-fermented) and Oolong tea (semi-fermented). Among them, 78% of the tea produced and consumed is black tea, which is consumed principally in North America, Europe, India and North Africa (except Morocco), 20% is green tea that is widely drunk in China, Japan, Korea and Morocco, and less than 2% is Oolong tea that is popular in Southern China. In addition, it exists a special tea named dark tea which is a unique microbial fermented tea, and its production and consumption is limited only to the areas of China and Japan (Chen and Sang 2014; Zheng et al. 2015). Theaflavin (TF1, Fig. 1a), theaflavin-3-gallate (TF2A), theaflavin-3′-gallate (TF2B) and theaflavin-3,3′-digallate (TF3), formed from the oxidation and polymerization of catechins during the manufacturing process of black tea, are the major theaflavins in black tea (Li et al. 2013). They contain a benzotropolone moiety as their core structure and contribute to the characteristic flavor and bright orange–red color of black tea. Furthermore, it has been reported that theaflavins possess various biological effects (Pan et al. 2013), such as antioxidant, anticancer, antihyperglycemic and anti-inflammatory activities. Nevertheless, the study on the in vivo activity of theaflavins is still limited up to date, and this question may be due to their unknown absorption, metabolism and bioavailability (Del et al. 2013). Additionally, dietary polyphenols especially in high concentrations exhibit adverse effects, such as inhibition of digestives enzymes, growth-rate depression, bodyweight decrease, and perturbation of mineral absorption from the alimentary canal (Rawel et al. 2006). Some of these properties may be directly or indirectly induced/caused by their interactions with proteins (Kroll et al. 2003; Papadopoulou et al. 2005). The binding of dietary polyphenols and proteins influences the structure of proteins, content of

✉ Xiaoxiong Zeng
zengxx@njau.edu.cn

[1] College of Food Science and Technology, Nanjing Agricultural University, Nanjing 210095, China
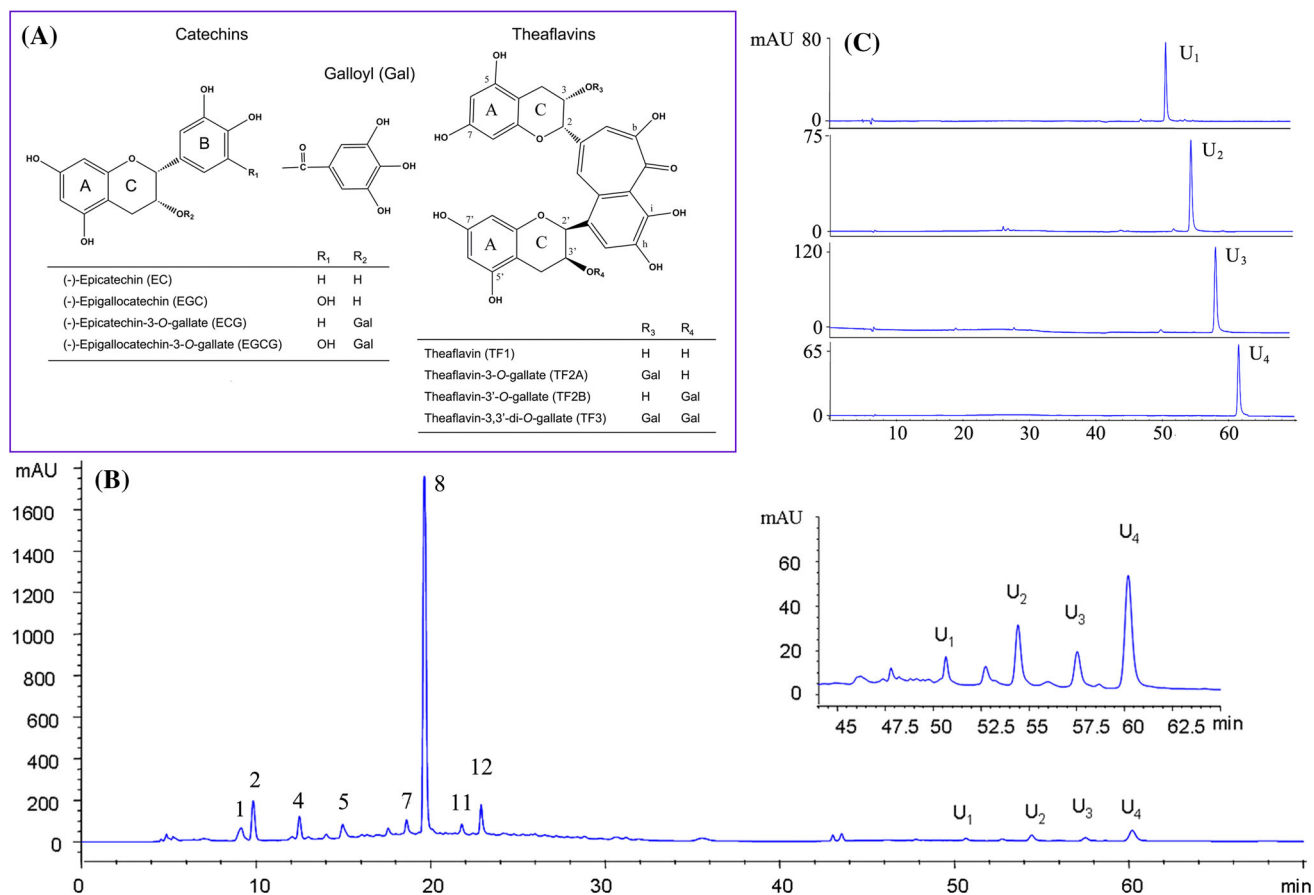
Fig. 1 Chemical structures of tea catechins and theaflavins (**a**), representative elution profile of extract from black tea by HPLC–DAD (**b**), and HPLC–DAD chromatograms and UV spectra of the fractions separated by AKTA purifier (**c**). Peaks: *1* 5-galloylquinic acid, *2* GA, *3* theobromine, *4* EGC, *5* EGCG, *6* caffine, *7* 4-*p*-coumaroylquinic acid, *8* ECG

free polyphenols, sensory quality of foods, antioxidants capacity and bioavailability of dietary polyphenols (Ozdal et al. 2013). Thus, the investigation of interactions between dietary polyphenols with proteins would help to understand their physiological fate so as to control the functional characteristics of foods.

Bovine serum albumin (BSA) as a model protein has been extensively studied in the interactions of polyphenolic compounds with protein (Soares et al. 2007). Recently, a number of studies were carried out on the interactions of tea catechins with BSA (Li and Hagerman 2014; Li and Hao 2015; Pal et al. 2012; Papadopoulou et al. 2005). However, the information on the interaction of theaflavins, being the dimers of a couple of epimerized catechins, with BSA is not available. Furthermore, fluorescence spectroscopy and circular dichroism (CD) spectroscopy gained wide acceptance for the determination of the interaction of phytochemical with protein (Li et al. 2015; Soares et al. 2007; Xu et al. 2015). This method possesses high sensitivity, rapidity and ease of implementation. It allows non-destructive measurements of substances in low concentration under various experimental conditions and provides

the binding information and reflects the conformation changes of proteins in various environments. Therefore, the aim of this study was to investigate the interactions of theaflavins with BSA by fluorescence and CD spectroscopy. Firstly, the theaflavins from various teas (green, Oolong, black and dark teas) were identified by liquid chromatography–electrospray ionization–mass spectrometry (LC–ESI–MS), and four individual theaflavins (TF1, TF2A, TF2B and TF3) were then purified from black tea. Finally, the interactions of the purified individual theaflavins with BSA were evaluated by fluorescence and CD spectroscopy in an attempt to characterize the chemical associations taking place.

Materials and methods

Materials and reagents

Tea samples of green, Oolong, black and dark teas were obtained from Yuhua Tea Factory (Nanjing, China), Orihiro Co., Ltd. (Takasaki-shi, Japan), Qimen Tea Factory

(Anhui, China) and Anhua Tea Factory (Hunan, China), respectively. Standards of (−)-epicatechin (EC, >98%), (+)-catechin (C, >98%), epigallocatechin (EGC, >98%), (−)-gallocatechin (GC, >98%), epicatechin-3-gallate(ECG, >98%), (−)-catechin gallate (CG, >98%), epigallocatechin-3-gallate (EGCG, >98%) and (−)-gallocatechin gallate (GCG, >98%) were purchased from Funakoshi Co., Ltd. (Tokyo, Japan). BSA (>96%), gallic acid (GA, >98%), caffeine (>98%), theobromine (>98%), high performance liquid chromatography (HPLC) grade of methanol and acetonitrile (MeCN) were obtained from Sigma Chemical Co. (St. Louis, MO, USA). Polyamide resin (80-100 mesh) was purchased from Sinopharm Chemical Reagent Co., Ltd. (Shanghai, China). HPLC grade of formic acid was purchased from Aladdin Industrial Inc. (Shanghai, China). Methanol-d4 (CD$_3$OD) for nuclear magnetic resonance (NMR) spectrometry was purchased from J&K Scientific Ltd. (Beijing, China).

Phosphate buffer solution (0.05 M) containing 0.1 M NaCl was used to keep the pH of the solution at 7.4. BSA stock solution was prepared with the phosphate buffer solution and kept in the dark at 4 °C. The stock solutions of theaflavins (1.0 mM) were prepared with double-distilled water (ddH$_2$O). All of other reagents were of analytical grade and ddH$_2$O was used throughout the experiments.

Preparation of tea infusion

Aqueous infusions of green, Oolong, black and dark teas were used as the source of tea catechins and theaflavin derivatives of HPLC–DAD (diode array detector) analysis. Firstly, all of these teas were ground into tea powders by a mill. Then, tea infusions of each sample were prepared by using two different methods. One (method A) was that 10.0 g tea powder was extracted three times by using 1000 mL ddH$_2$O at 90 °C for 30 min in dark. Another one (method B) was that pouring 100 mL 50% methanol solution over 1.0 g tea powder and brewing in a water bath at 70 °C for 30 min with stirring (120 rpm) in dark. After brewing, 50 mL of each infusion was mixed with 1.0 mL acetic acid in order to bring down pH and stabilize polyphenols prior to analysis. After filtration through a 0.45 μm cellulose/nylon filter, the filtrate was immediately analyzed by HPLC–DAD.

Preparation of TF1, TF2A, TF2B and TF3

For preparation of monomers of theaflavins, 10.0 g black tea powder was extracted three times by using 300 mL ddH$_2$O at 90 °C for 30 min in dark. After brewing, the whole infusion was acidified and centrifuged. The supernatant was collected and applied to a column (30 × 1.6 cm) of ployamide resin. After reaching adsorptive saturation, the column was first washed with 5 times of bed volume (BV) of deionized water, and then was eluted by 5 times of BV of 80% ethanol–water solution (80:20, v/v), finally was eluted by ethanol–water–ethyl acetate solution (4:1:5, v/v/v). The ethanol–water–ethyl acetate elution was collected and concentrated, affording crude product of theaflavins (about 60% for total theaflavins) for further purification.

The crude product of theaflavins was dissolved in 50% aqueous methanol (v/v). After filtration through a 0.45 μm nylon filter, the filtrate was applied to YMC-Pack ODS-A column (250 × 20 mm, 5 μm, YMC, Kyoto, Japan) equipped with an AKTA purifier system (GE Healthcare Bioscience, Piscataway, NJ, USA). The column was eluted by MeCN–water–ethyl acetate solution (7:17:1, v/v/v; pH 2.5, adjusted with formic acid) at a flow rate of 1.5 mL/min, and the elution was detected at 280 nm with an ultraviolet (UV) detector. The fractions were auto-collected (3 mL/tube) and analyzed by HPLC–DAD, and the fractions containing the desired theaflavins were collected, concentrated and freeze-dried by a Freeze-Dry System (Labconco, Kansas City, MO, USA), respectively, affording TF1, TF2A, TF2B and TF3.

Structural identification of TF1, TF2A, TF2B and TF3 prepared

The structures of TF1, TF2A, TF2B and TF3 prepared were confirmed by ESI–time-of-flight–MS (ESI–TOF–MS) and ^{1}H NMR. ESI–TOF–MS spectra were recorded on an Applied Biosystems Mass Spectrometer. ^{1}H NMR spectra in CD$_3$OD as solvent were recorded with a Bruker DRA-500 Spectrometer operated at 300 K. Coupling constants are expressed in hertz, and chemical shifts are given on a δ (parts per million, ppm) scale with tetramethylsilane as an internal standard.

HPLC–DAD and HPLC–MS analysis

HPLC–DAD analysis was done on an Agilent 1100 series HPLC system (Agilent Technologies, Santa Clara, CA, USA). The separation was achieved with a TSK-gel ODS-80 TSQA column (250 × 4.6 mm, 5 μm, Tosoh, Japan). The temperature of column oven was set at 40 °C. The DAD acquisition wavelength was set in the range of 200–800 nm, and the detector was set at 280 nm for detection of tea catechins, purine alkaloids and theaflavins. The mobile phase consisted of methanol (A), 12.5% ethyl acetate/MeCN solvent (B) and solvent of 0.2% formic acid/water (C). The flow rate was set at 0.6 mL/min. The injection volume was 20 μL. After sample injection, elution was performed with the linear gradient as follows: 15%/0%/85% of A/B/C at 0 min, 45%/0%/55% of A/B/C

at 20 min, 45%/0%/55% of A/B/C at 25 min, 0%/23%/ 77% of A/B/C at 35 min, 0%/28%/72% of A/B/C at 70 min, and 0%/45%/55% of A/B/C at 85 min. Each peak of theaflavins was preliminarily confirmed by an Agilent 1100 HPLC equipment coupled with an ESI–MS system. The molecular weights of theaflavins were analyzed in negative ionization mode. LC–MS conditions were as follows: column, TSK-gel ODS-80 TSQA column; flow rate, 0.6 mL/min; injection volume, 20 μL; column temperature, 40 °C; probe voltage, + 4.5 V (ESI-negative mode); nebulizer gas flow, 1.5 L/min; drying gas pressure, 0.1 MPa; CDL temperature, 350 °C.

Fluorescence measurement

Appropriate quantities of 1.0×10^{-4} M theaflavins (TF1, TF2A, TF2B and TF3) and EGCG solution were transferred to 10 mL flasks, respectively, and then 1.0 mL of BSA solution was added and the mixtures were diluted with phosphate buffer to 10.0 mL. The resultant mixtures were subsequently incubated at 20 or 37 °C for 15 min. Then, the fluorescence spectra were recorded by using F-7000 fluorescence spectrophotometer (Hitachi High-Technologies Corp., Tokyo, Japan) in the wavelength range of 290–500 nm by setting the excitation at 280 nm and excitation and emission bandwidths at 5 nm. Each spectrum was the mean of at least three scans.

The three-dimensional (3D) fluorescence spectra of BSA in absence and presence of EGCG/theaflavins were recorded with the setting of the excitation and the emission wavelength range of 200–600 nm with an interval of 5 nm, respectively.

Synchronous fluorescence spectra of BSA in the absence and presence of EGCG/theaflavins were determined at different scanning intervals of $\Delta\lambda$ ($\Delta\lambda = \lambda_{em} - \lambda_{ex}$), $\Delta\lambda = 15$ nm and $\Delta\lambda = 60$ nm, where the spectrum only revealed the spectroscopic characteristic of Tyr and Trp residues in BSA, respectively. Specifically, the excitation wavelength was set in the range of 250–320 nm, and thus the emissions were recorded from 265 to 335 nm for Tyr residues and 310–380 nm for Trp residues of BSA, respectively. Each scan was carried out in triplicate to get mean values and the buffer solution signal was used as reference for data correction.

CD measurement

The CD spectra of BSA and its complexes with TF3 or EGCG were made on a Jasco-810 spectrophotometer (JASCO Corp., Tokyo, Japan), using a 1 mm cell with three scans averaged for each CD spectra at room temperature. The spectra were recorded in far-UV region (190–250 nm) and the scan rate was 50 nm/min with a

response time of 4 s. All samples were prepared in 10 mM phosphate buffer (pH 7.4). The BSA concentration was set at 1.0×10^{-6} M and the complexes were prepared by mixing BSA with TF3 or EGCG at a molar ratio of 1:20, 1:40 and 1:80 (BSA to TF3 or EGCG). To obtain the secondary contents of BSA, curvefitting programme software CDPro with CONTIN, SELCON and CDSSTR methods was employed to analyze the CD data (Sreerama and Woody 2000).

Results and discussion

Isolation, purification and identification of TF1, TF2A, TF2B and TF3

Figure 1b shows the HPLC chromatogram of a black tea infusion, and peaks 1, 2, 4, 5, 7, 8, 11 and 12 were identified as 5-galloylquinic acid, GA, theobromine, EGC, EGCG, caffeine, 4-*p*-coumaroylquinic acid, and ECG, respectively, according to retention times, online DAD spectra of authentic standards, mass data and literature (Clifford et al. 2003; Kiehne and Engelhardt 1996; Wang et al. 2008a). In addition, four unknown peaks (U₁, U₂, U₃ and U₄), possible being theaflavins, were observed. In order to identify the structures of these four peaks, the crude extract was isolated from the black tea infusion by column chromatography of polyamide resin and then purified by a semi-preparative column of YMC-Pack ODS-A performed on an AKTA purifier. The fractions containing U₁, U₂, U₃ and U₄ were obtained and analyzed by HPLC–DAD (Fig. 1c). As results, the purity was 95.1% for U₁, 96.3% for U₂, 98.4% for U₃, and 98.8% for U₄. Then, the structures of U₁, U₂, U₃ and U₄ were characterized by ESI–TOF–MS and ¹H NMR.

Data for U₁: ¹H NMR (500 MHz, CD₃OD, TMS internal reference), δ 7.96 (s, 1H), 7.83 (s, 1H), 7.34 (s, 1H), 6.01 (d, $J = 2.3$ Hz, 1H), 5.98 (d, $J = 2.3$ Hz, 1H), 5.96 (dd, $J = 2.5, 5.7$ Hz, 2H), 5.62 (s, 1H), 4.91 (brs, 1H), 4.45 (d, $J = 2.4$ Hz, 1H), 4.31 (s, 1H), 3.01–2.90 (m, 2H), 2.82 (m, 2H); ESI–MS, *m/z* 562.9 for [M–H]⁻. Data for U₂: ¹H NMR (500 MHz, CD₃OD, TMS internal reference), δ 7.90 (s, 1H), 7.78 (s, 1H), 7.37 (s, 1H), 6.80 (s, 2H), 6.04–5.98 (m, 4H), 5.78 (s, 1H), 5.54 (s, 1H), 5.10 (s, 1H), 4.17 (d, $J = 2.4$ Hz, 1H), 3.04 (m,2H), 2.88 (m, 2H); ESI–MS, *m/z* 715.0 for [M–H]⁻. Data for U₃: ¹H NMR (500 MHz, CD₃OD, TMS internal reference), δ 7.86 (s, 2H), 7.35 (s, 1H), 6.84 (s, 2H), 6.07 (d, $J = 2.3$ Hz, 1H), 6.00 (d, $J = 2.4$ Hz, 1H), 5.98 (brs, 2H), 5.82 (s, 1H), 5.60 (s, 1H), 4.93 (s, 1H), 4.24 (s, 1H), 3.10–2.84(m, 4H); ESI–MS, *m/z* 715.0 for [M–H]⁻. Data for U₄: ¹H NMR (500 MHz, CD₃OD, TMS internal reference), δ 7.79 (s, 1H), 7.75 (s, 1H), 7.47 (s, 1H), 6.88 (s, 2H), 6.80 (s, 2H), 6.07–6.01 (m,

4H), 5.86 (s, 1H), 5.76 (brs, 1H), 5.67 (d, $J = 2.7$ Hz, 1H), 5.20 (s, 1H), 3.08–3.20 (m, 2H), 2.94–2.90 (m, 2H); ESI–MS, m/z 866.9 for [M–H]$^-$. These data are in accordance with the previous literature (Wang et al. 2008b). Simultaneously referring to the retention time, absorbance spectrum in HPLC–DAD analysis, U_1, U_2, U_3 and U_4 were identified as TF1, TF2A, TF2B and TF3, respectively.

Identification and quantification of major components in tea infusions

The polyphenolic compounds in tea infusions were identified on the basis of their retention times, absorbance spectra, m/z of their quasi-molecular ions, MS^2 fragmentation patterns with those of the authentic standards and the literature data. It should be noted that a number of phenolics found in teas were not available in a purified form. However, in most instances, compounds could be identified on the basis of MS fragmentation data coupled with characterization in previously published studies (Kuhnert et al. 2010; Menet et al. 2004; Wang et al. 2008a). Figure S1 shows the representative chromatograms of infusions from green, Oolong, and dark teas prepared by method B, and that of black tea is the same to that in Fig. 1b, where U_1, U_2, U_3 and U_4 were identified. Table S1 shows the retention times, MS and MS^2 data and the identification results for the peaks numbered in the chromatograms. As mentioned above, peaks 2, 3, 4, 5, 6, 7, 8, 9, 10, 12 and 13 were identified as GA, GC, theobromine, EGC, C, EGCG, caffine, EC, GCG, ECG and CG, respectively. Peak 1 was identified by MS and MS^2 data as 5-galloylquinic acid (theogallin), which has previously been characterized and detected in significant quantity in green tea (Wang et al. 2008a) because authentic standard was not available. However, MS analysis of the peak revealed a [M–H]$^-$ ion at m/z 343 that fragmented to yield a MS^2 spectrum with ions at m/z 190.8, the amu of a quinic acid, and m/z 169, which corresponds with GA. Peak 11 had a similar absorbance spectrum but different HPLC retention time to p-coumaric acid, and MS analysis yielded a [M–H]$^-$ at m/z 337 and a prominent MS^2 ion at m/z 172.8, which, in accordance with that reported by Clifford et al. (2003), matches the mass spectrum of 4-p-coumaroylquinic acid, a known component of black tea (Kiehne and Engelhardt 1996).

In the present study, nine catechins, two purine alkaloids, two quinic acids and four theaflavin derivatives (TF1, TF2A, TF2B and TF3) were identified as described above. Based on the identification results, quantification of the major components was accordingly performed by using the external standard method. However, the amounts of 5-galloylquinic acid and 4-p-coumaroylquinic acid were not quantified because of the lack of the corresponding reference compounds. For determination, calibration curves were obtained at a detection wavelength of 280 nm for nine catechins, two purine alkaloids and four theaflavin derivatives by using standard solutions at six different concentration levels. As shown in Table S1, all calibration curves were linear over the concentration ranges tested with good correlations.

Using the developed HPLC–DAD method, the contents of tea catechins, purine alkaloids and four theaflavin derivatives in green, black, Oolong and dark teas were determined and the results are listed in Table S2. The tea infusions were prepared by two different methods as mentioned in Sect. 2.2. Quantification was based on mean peak areas for each compound obtained for assessment of intraday variability (n = 5). Notably, green tea contained higher levels of tea catechins than black and dark teas ($P < 0.05$), but the values were considerably close to those of Oolong tea which is semi-fermented tea ($P > 0.05$). TF1, TF2A, TF2B and TF3 were not detected in green tea, Oolong and dark teas contained lower levels of theaflavin derivatives, but all four theaflavin derivatives were detected in black tea in concentrations ranging from 0.27 to 1.48 mg/g. Green tea is derived directly from inactivating the activity of polyphenol oxidase (PPO) by steaming or microwave and drying the fresh tea leaves, thus, the chemical composition of green tea is very similar to that of fresh tea leaves. For black and dark teas, most of tea catechins are oxidized and polymerized by endogenous or microbial enzymes during the manufacturing process. As Oolong tea is a partially fermented tea, it has relatively higher level of tea catechins and lower level of theaflavin derivatives than black tea. Furthermore, it was found that the concentrations of four theaflavin derivatives were much higher in tea infusion prepared by method B than in infusion prepared by method A. The contents of TF1, TF2A, TF2B and TF3 per gram black tea extracted by method B were 0.83, 1.04, 0.65 and 1.48 mg, respectively, while the contents per gram black tea prepared by method A were 0.54, 0.71, 0.27 and 0.99 mg, respectively. Therefore, method B (50% aqueous methanol at 70 °C) showed better extraction efficiency than method A (hot water at 90 °C) for theaflavin derivatives ($P < 0.05$). It might be due to that theaflavin derivatives contain the hydrophobic moiety, a bis-flavan-substituted 1′,2′-dihydroxy-3,4-benzptroplone moiety, resulting in that theaflavin derivatives showed a better solubility in 50% aqueous methanol than in water.

Fluorescence quenching of BSA by theaflavins

In the present study, fluorescence spectroscopy was employed to investigate the interactions between BSA and theaflavins. Generally, the BSA fluorescence is derived from phenylalanine (Phe), Tyr and Trp residues, and Trp

residues mainly provide intrinsic fluorescence of BSA (Li et al. 2011). During the course of the experiment, all fluorescence emissions from EGCG, theaflavins, buffer and other reagents were feeble, hence their impacts on fluorescence analysis could be negligible. As shown in Fig. 2, the fluorescence of BSA was quenched by using various concentrations of EGCG and theaflavins. It was observed that the fluorescence intensity of BSA dropped regularly with the increase of EGCG/theaflavins concentration, which indicated the occurrence of interaction between EGCG/theaflavins and BSA. A slight red shift of maximum emission wavelength (from 342 to 346 nm) was observed
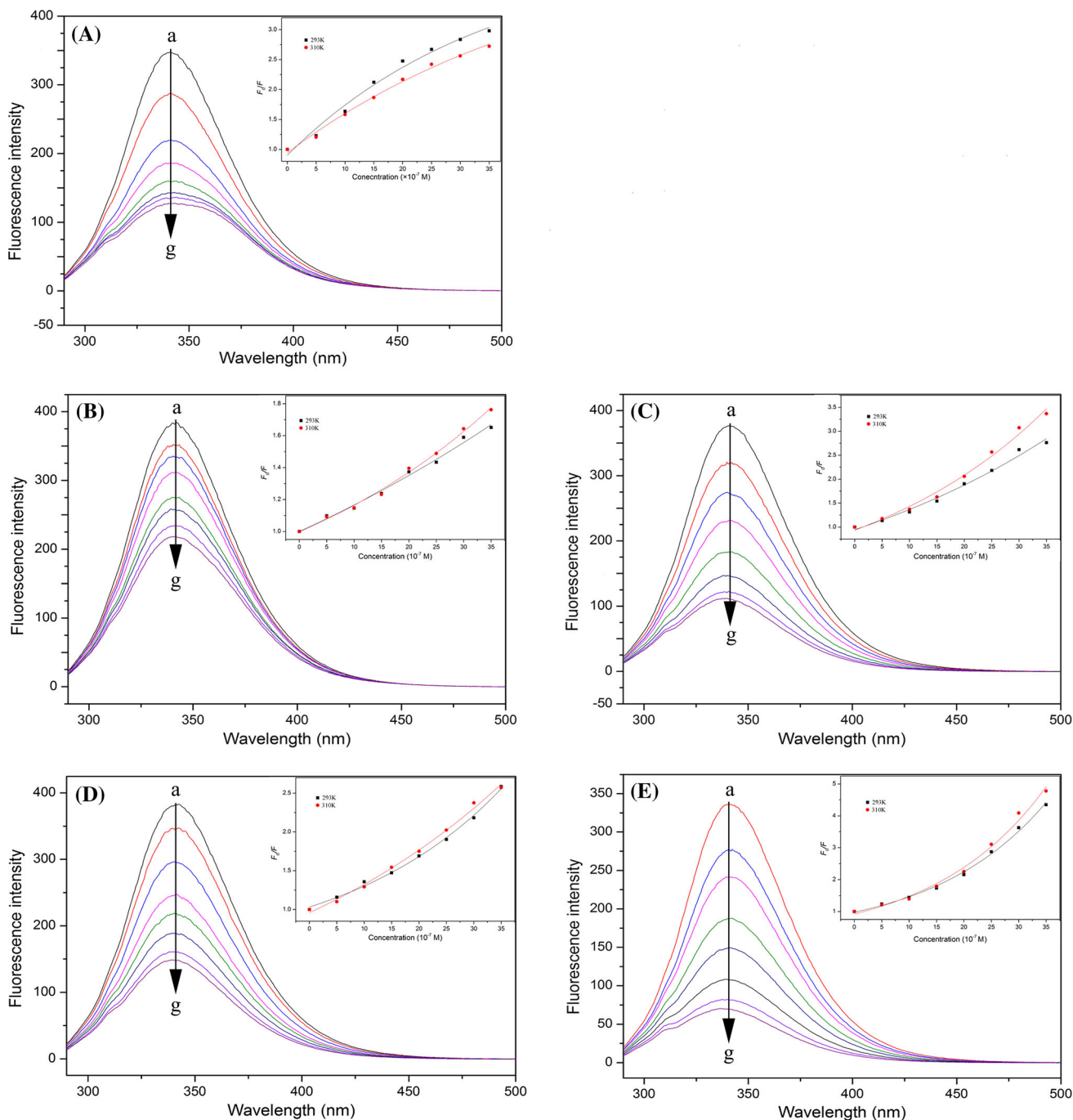

Fig. 2 Fluorescence emission spectra of BSA in the presence of various concentrations of EGCG (**a**), TF1 (**b**), TF2A (**c**), TF2B (**d**) and TF3 (**e**). Conditions: temperature, 37 °C; λ_{ex}, 280 nm; BSA, 1×10^{-6} mol/L; EGCG or theaflavins, 0.5, 1.0, 1.5, 2.0, 2.5, 3.0 and 3.5×10^{-6} M (*a–g*). The *inset* corresponds to Stern–Volmer plots for the quenching of BSA by EGCG and theaflavins (temperature, 293 and 310 K, $\lambda_{ex} = 280$ nm)

for EGCG, implying that the secondary structure of BSA changed (Pal et al. 2012). However, theaflavins just caused a concentration-dependent quenching of the intrinsic fluorescence intensity of BSA without changing the emission maximum and shape of the peaks (Fig. 2b–e).

The following Stern–Volmer equation can describe the correlativity between fluorescence quenching intensity with quencher concentration (Lakowicz 2006).

$$\frac{F_0}{F} = 1 + K_q\tau_0[Q] = 1 + K_{sv}[Q] \tag{1}$$

where F_0 and F are the fluorescence intensities of BSA in the absence and presence of quencher, $[Q]$ is the quencher concentration, K_q is the biomolecule quenching constant, τ_0, with a value of 10^{-8} s, is the average life-time of fluorescence without quencher and K_{sv}, given by $K_q\tau_0$, is the Stern–Volmer quenching constant. Fluorescence intensities were read at emission wavelength of 342 nm where the emission maximum of BSA was located. The Eq. (1) was applied to determine K_q by linear regression of plots of F_0/F versus $[Q]$. When a linear Stern–Volmer plot is generated, it is an indication of a single class of fluorophores in a protein, which are all equally accessible to the quencher. This also means that only one mechanism of quenching, either dynamic or static occurs. However, multiple fluorophores such as BSA generate negative deviations in Stern–Volmer equation. In a classic model, values of F_0/F increase linearly with $[Q]$, while here they showed downward tendency toward the x-axis at high $[Q]$, indicating differences in the accessibilities of fluorophores to the quencher (Li and Hagerman 2014). In the modified Stern–Volmer equation (Eq. 2), a factor for fractional accessibility f_a is included. It allows calculation for the modified Stern–Volmer constant K for systems having more than one fluorophore.

$$\frac{F_0}{F_0 - F} = \frac{1}{f_a} + \frac{1}{f_a K[Q]} \tag{2}$$

In several cases, the same quencher can quench the fluorophore by both collision and complex formaton mechanisms. While in other cases, an upward curvature indicates a sphere of action existing. This assumes that a sphere of volume exists around a fluorophore, within which a quencher will cause quenching with a probability of 1. In this case, the Stern–Volmer plot shows an upward curvature, concave toward the y-axis at high $[Q]$, and Stern–Volmer equation is modified to the following form in which F_0/F is related to $[Q]$.

$$\frac{F_0}{F} = (1 + K[Q])\exp([Q]VN/1000) \tag{3}$$

In this equation, N is the Avogadro's constant while V is the volume of the sphere. If $K[Q]$ is small enough,

$(1 + K[Q]) \approx \exp(K[Q])$, which is equivalent to $\exp([Q]VN)$ (Soares et al. 2007). Thus, the preview equation changes to Eq. (4).

$$\frac{F_0}{F} = e^{(K[Q])} \tag{4}$$

Figure 2 also shows the Stern–Volmer plots for the BSA fluorescence quenching by EGCG/theaflavins. The Stern–Volmer plot of EGCG was linear at low concentrations, but it revealed a small downward concave toward the x-axis at higher concentrations (Fig. 2a). The results indicated the quenching of Trp212 fluorescence (buried in the hydrophobic pocket) in BSA by EGCG (Li and Hagerman 2014). In this case, BSA fluorescence quenching by EGCG obeyed the modified form of the Stern–Volmer equation (Eq. 2) as described previously (Fig. 3a). For theaflavins, the Stern–Volmer plot exhibited an upward curvature and was concaved toward the y-axis at high concentrations (Fig. 2b–e). As previously mentioned, this characteristic feature could mean that BSA can be quenched by both mechanisms (static and dynamic quenching), indicating that both Trp residues (Trp134 and Trp212) binding occurs (Wei et al. 2006). In this case, the quenching of BSA fluorescence by theaflavins obeyed the modified form of the Stern–Volmer equation (Eq. 4) (Fig. 3b–e).

Stern–Volmer plot of EGCG/theaflavins exhibited the same trends under different temperatures. The values of K_{sv}/K_{app} and K_q for the interactions of EGCG/theaflavins with BSA at two temperatures (293 and 310 K) are shown in Table 1. The values of K_q for all tested systems are higher than the maximum scatter collision quenching constant (2.0×10^{10} M^{-1} s^{-1} for dynamic quenching) of various quenchers with the fluorophore (BSA), confirming that the static quenching mechanism is the main reason of protein fluorescence quenching (Ware 1962). Furthermore, the values of K_q and K_{sv} were inversely correlated with temperature for EGCG, which again indicated that the nature of quenching was static (Xu et al. 2013), resulting from the formation of EGCG–BSA complex. However, the increases of K_{app} and K_q values were observed by increasing temperature in case of theaflavins. Considering that K_q values of the BSA quenching procedure initiated by theaflavins were much higher than 2.0×10^{10} M^{-1} s^{-1}, the probable quenching mechanism for theaflavins was both dynamic and static (Zhao et al. 2006). The highest value of K_q was determined at 37 °C (310 K) for TF3 and K_q decreased in the order of TF3 > TF2A > TF2B $\approx$ EGCG > TF1.

Synchronous fluorescence spectroscopy is the most common technique for the investigation of the microenvironment of amino acid residues in protiens (Simion et al. 2015). The synchronous fluorescence can provide the characteristic information of Tyr or Trp residues in BSA
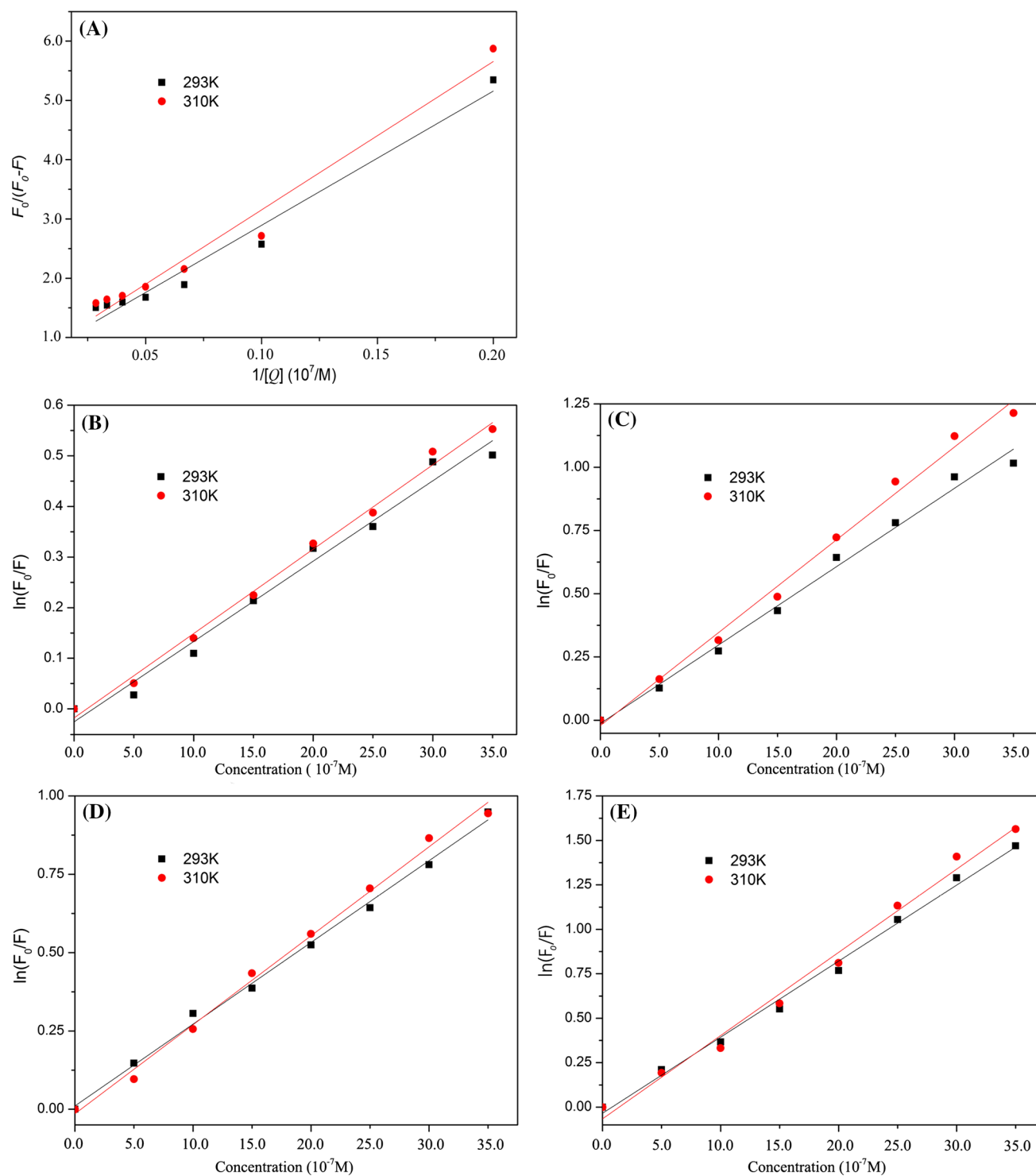
Fig. 3 Modified Stern–Volmer plots for the quenching of BSA by EGCG and theaflavins (temperature, 293 and 310 K, $\lambda_{ex} = 280$ nm). **a** modified Stern–Volmer plots for EGCG-mediated quenching of BSA fluorescence (Eq. 2); **b** modified Stern–Volmer plots for TF1-mediated quenching of BSA fluorescence (Eq. 4); **c** modified Stern– Volmer plots for TF2A-mediated quenching of BSA fluorescence (Eq. 4); **d** modified Stern–Volmer plots for TF2B-mediated quenching of BSA fluorescence (Eq. 4); **e** modified Stern–Volmer plots for TF3-mediated quenching of BSA fluorescence (Eq. 4)

according to the D-value ($\Delta\lambda$) between excitation wavelength and emission wavelength, set at 15 or 60 nm, respectively (Liu et al. 2015; Zhang et al. 2008). As shown

in Fig. S2, the fluorescence intensity of BSA weakened regularly along with the addition of EGCG/theaflavins. The maximum emission wavelength showed a weak red shift

Table 1 The Stern–Volmer quenching constants (K_{sv}), apparent static quenching constants (K_{app}), bimolecular quenching constants (K_q), binding constants (K_a) and relative thermodynamic parameters for the interactions of EGCG/theaflavins with BSA at different temperatures

Sample	Temperature (K)	$F_0/F - [Q]$			$lg[(F_0 - F)/F] - lg[Q]$[a]	K_a (×10^6 L mol^{-1})	n	ΔG^0 (kJ mol^{-1})	ΔH^0 (kJ mol^{-1})	ΔS^0 (J mol^{-1} k^{-1})
			K (10^5 M^{-1})	K_q (10^{13} M^{-1} s^{-1})						
EGCG[b]	293	$y = 22.64x + 0.6275$ ($R^2 = 0.9761$)	2.77	2.77	$y = 1.1242x + 6.6146$ ($R^2 = 0.9937$)	4.12	1.12	−37.74	41.85	267.08
	310	$y = 25.04x + 0.6478$ ($R^2 = 0.9817$)	2.58	2.58	$y = 1.1981x + 6.8986$ ($R^2 = 0.9913$)	7.92	1.20	−35.44		
TF1[c]	293	$lny = 158771x - 0.0257$ ($R^2 = 0.9934$)	1.59	1.59	$y = 1.1523x + 6.2123$ ($R^2 = 0.9891$)	5.16	1.15	−38.29	31.58	234.47
	310	$lny = 166731x - 0.018$ ($R^2 = 0.9897$)	1.67	1.67	$y = 1.1312x + 6.3266$ ($R^2 = 0.9967$)	8.45	1.13	−41.11		
TF2A[c]	293	$lny = 309803x - 0.0128$ ($R^2 = 0.9825$)	3.10	3.10	$y = 1.2365x + 7.1449$ ($R^2 = 0.9979$)	13.96	1.24	−40.76	15.43	188.55
	310	$lny = 366957x - 0.021$ ($R^2 = 0.9899$)	3.67	3.67	$y = 1.2482x + 7.2496$ ($R^2 = 0.9975$)	17.77	1.25	−43.02		
TF2B[c]	293	$lny = 260913x + 0.0106$ ($R^2 = 0.9952$)	2.61	2.61	$y = 1.2455x + 7.0936$ ($R^2 = 0.9961$)	12.41	1.25	−40.47	14.44	184.26
	310	$lny = 284030x - 0.0144$ ($R^2 = 0.9841$)	2.84	2.84	$y = 1.2645x + 7.1916$ ($R^2 = 0.9899$)	15.55	1.26	−42.68		
TF3[c]	293	$lny = 427620x - 0.0343$ ($R^2 = 0.9867$)	4.28	4.28	$y = 1.2566x + 7.2297$ ($R^2 = 0.9897$)	16.97	1.26	−41.24	15.89	191.72
	310	$lny = 486809x - 0.1128$ ($R^2 = 0.9931$)	4.87	4.87	$y = 1.2733x + 7.3375$ ($R^2 = 0.9843$)	21.75	1.27	−43.54		

[a] The quencher concentrations ranged from 5 × 10^{-7} to 20 × 10^{-7} M

[b] Estimated as K_{sv} from modified Stern–Volmer plot (Eq. 2)

[c] Estimated as K_{app} from modified Stern–Volmer plot (Eq. 4)

($\sim$2.0 nm) for the addition of EGCG at $\Delta\lambda = 60$ nm. The result indicated that EGCG bonded to BSA and located in closed proximity to the Trp residues, the polarity near the Trp residues was increased and thus the hydrophilicity was increased obviously (Li and Hao, 2015). At $\Delta\lambda = 15$ nm, slight blue shift of the maximum emission wavelength ($\sim$2 nm) for EGCG/TF2A/TF2B/TF3 were observed. These changes suggested that the hydrophobic part of TF3, TF2A, TF2B and EGCG molecules was close enough to the phenyl moiety of Tyr, thus the hydrophobicity near the Tyr residues increased. With the addition of TF1 to BSA, there was no significant shift of the maximum emission wavelength at $\Delta\lambda = 15$ or 60 nm, implying that the interaction of TF1 with BSA could not affect the microenvironment around the Tyr or Trp residues. These results provided an interesting observation that both the molecular skeleton and number of galloyl moiety of quenchers greatly affected the microenvironment around the Tyr and Trp residues of BSA, which is in good accordance with the quenching constants of theaflavins and EGCG obtained from fluorescence spectroscopy.

In recent years, the 3D fluorescence spectra have been extensively employed to explore the characteristic conformational change of protein (Roy et al. 2013). In the present study, the 3D spectra of BSA and the mixtures of BSA with EGCG/theaflavins showed two distinct peaks in BSA marked peaks 1 ($\lambda_{ex}/\lambda_{em}$, 280/340 nm) and 2 ($\lambda_{ex}/\lambda_{em}$, 230/340 nm). Peak 1 reveals the spectral characteristics of Trp and Tyr residues and peak 2 corresponds to the spectral properties of the polypeptide backbone which is mainly attributed to the presence of the π–π* and n–π* transitions, respectively. Addition of EGCG and theaflavins dcreased the flourescence intensity in both peaks. Peak 2 showed a red shift of 20 nm and a blue shift of 10 nm in the BSA with addition of EGCG and TF3, respectively (Table 2). It was found that the quenching effect showed a sequence as TF3 > TF2A > TF2B > EGCG > TF1, which is in accordance with the results of fluorescence experiments. The difference of effect might be due to the structural difference of TF3, TF2A, TF2B and TF1 (Fig. 1a), suggesting the important roles of the gallate moat the C-3 position and hydrophobic interaction between the aromatic ring and the hydrophobic moiety.

Fluorescence binding constant and binding site

The binding constant (K_a) and the number of binding sites (n) for the interaction of theaflavins/EGCG and BSA can be obtained by the following Eq. (5) (Lakowicz 2006). The values of n and K_a can be calculated by the slope and intercept with the plots of $\log[(F_0 - F)/F]$ against $\log[Q]$.

$$\log[(F_0 - F)/F] = \log K_a + n \log[Q] \tag{5}$$

Table 2 Three-dimensional fluorescence spectral characteristic parameters of BSA, BSA–EGCG and BSA-theaflavins systems at 37 °C

System	Peak 1 (nm)		Intensity	Peak 2 (nm)		Intensity
	λ_{ex}	λ_{em}		λ_{ex}	λ_{em}	
BSA	280	340	411.50	230	340	237.30
BSA-EGCG	280	340	181.40	230	350	97.84
BSA-TF1	280	340	203.29	230	340	108.10
BSA-TF2A	280	340	96.35	230	340	43.79
BSA-TF2B	280	340	152.50	230	340	77.75
BSA-TF3	280	340	74.31	230	330	33.34

To obtain K_a and n per protein, the fluorescence quenching data were analyzed according to the Eq. (5) at low quencher concentrations from 5×10^{-7} to 20×10^{-7} M. The results are summarized as shown in Table 1. The results demonstrated that K_a was in the order of TF3 > TF2A > TF2B > TF1 > EGCG, indicating that introduction of galloyl moiety into TF1 (resulting in TF2A, TF2B and TF3) enhanced the binding affinity of TF2A, TF2B and TF3 with BSA. Furthermore, the binding affinity increased with the increase of molecular weight of quencher and the presence of the galloyl moiety on the C-3 position of theaflavins. As compared with tea catechin-BSA or human serum albumin (HSA) interactions with K_a from 10^3 to 10^6 M^{-1} (Pal et al. 2012; Soares et al. 2007; Trnková et al. 2011), the K_a values (10^6–10^7 M^{-1}) for interactions of theaflavins and BSA were high, indicating comparatively strong ligand–protein interactions. The value of n for the interaction of ligand and BSA approximately equal to 1, indicating that the existence of just a single binding site in BSA for theaflavins/EGCG. Furthermore, it is suggested that theaflavins/EGCG most likely binds to hydrophobic pocket locate in sub-domain IIA (Sułkowska 2002).

Thermodynamic parameters and binding mode

It is important that the thermodynamic parameters, ΔH^0 (enthalpy change), ΔS^0 (entropy change) and ΔG^0 (free energy change), which can be used to propose the binding mode. Considering that the ΔH^0 does not vary significantly over the temperature range, it can be considered as a constant. ΔH^0 and ΔS^0 can be calculated using the Van't Hoff equation:

$$\ln K = -\frac{\Delta H^0}{RT} + \frac{\Delta S^0}{R} \tag{6}$$

$$\ln(K_2/K_1) = (1/T_1 - 1/T_2)\Delta H^0/R \tag{7}$$

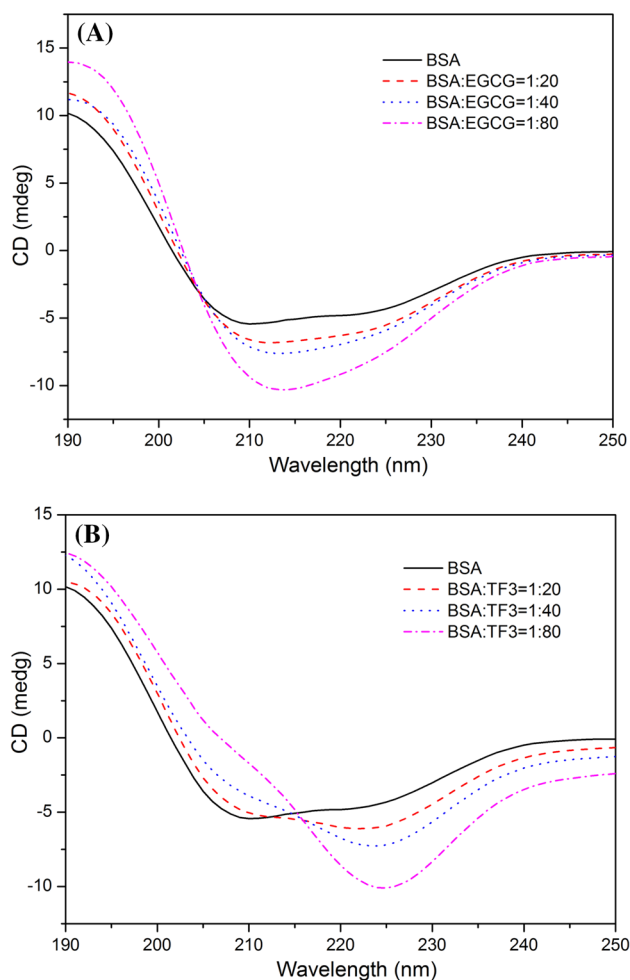$$\Delta G^0 = \Delta H^0 - T\Delta S^0 \tag{8}$$

Fig. 4 Circular dichroism spectra of free BSA and BSA-quencher complex. The free BSA and BSA-quencher complex in phosphate buffer solution with a protein concentration of 1×10^{-6} M and quencher concentrations of 2.0×10^{-5}, 4.0×10^{-5} and 8.0×10^{-5} M

where R is the gas constant and T is the experimental temperature, K is the binding constant at the corresponding T. Then ΔH^0, ΔS^0 and ΔG^0 of interaction can be calculated from the equations above.

The active force between phenolic compounds and biomolecules may include electrostatic interactions, van der Waals interactions, and hydrophobic effect and so on. As mentioned above, the model of interaction between quencher and a protein molecule can be concluded according to ΔH^0 and ΔS^0 data (Li et al. 2015). More specifically, (1) $\Delta H^0 > 0$ and $\Delta S^0 > 0$, the main force would be hydrophobic effect; (2) $\Delta H < 0$ and $\Delta S > 0$, it would be electrostatic force; (3) $\Delta H^0 < 0$ and $\Delta S^0 < 0$, it would be hydrogen bond and van der Waals interactions. In the present study, the thermodynamic parameters calculated by using the van't Hoff equation are presented in Table 1. It is evident that hydrophobic forces played a

significant role in the bindings of EGCG/theaflavins to BSA according to the both positive values of ΔH and ΔS (Xu et al. 2015). Furthermore, the negative values of ΔG^0 for all studied interactions suggested that the binding reaction was spontaneous.

CD spectra

Far UV (250–190 nm) CD spectroscopy was employed to investigate the influence of EGCG and TF3 on the secondary structure of BSA. The results are shown in Fig. 4 and Table S3. Two negative bands at 208 and 222 nm are the typical feature of α-helix structure in the CD spectrum of BSA (Greenfield 2006). To obtain the fractional contents of the secondary structure elements (α-helix, β-sheet, turns and unordered) of BSA in the absence and presence of EGCG or TF3, the CD spectra data were calculated by the CDPro software package. The secondary structure proportions for free BSA were α-helix 52.6%, β-sheet 7.9%, turns 15.2% and unordered 26.0%. With the addition of EGCG to BSA, the α-helix content increased to 76.7%, while the β-sheet content decreased to 0, and the unordered structure contents decreased to 15.3%, which is similar to the interactions of genistein with BSA (Roy et al. 2013). The results indicated that binding of EGCG to BSA induced stabilization of α-helix structure, the protein to be exposed to a more hydrophobic environment. But for the interaction of TF3 with BSA, the α-helix content decreased to 43.9%, while the β-sheet content increased to 19.6%, and the unordered structure content decreased to 15.5%. The decrease in α-helix content and increase in content of β-sheet indicated that TF3 could change the skeleton structure of BSA and induce the unfolding of BSA secondary structure. The results suggested that TF3 in high concentrations might possess a toxic effect on BSA, and the effects of TF3 and EGCG on secondary structure contents of BSA were significantly different.

Conclusion

In the present study, the structural identification of major compounds in green, Oolong, black and dark teas, including nine catechins, two purine alkaloids, two quinic acids and four theaflavin derivatives, were achieved using LC–ESI–MS. Monomers of TF1, TF2A, TF2B and TF3 with high purity (>95%) were successfully prepared from black tea by water extraction and followed by polyamide column chromatography and semi-preparative HPLC chromatography. Furthermore, the interactions of theaflavins with BSA were detected by fluorescence and CD spectroscopy. It was found that static quenching was most likely involved in the quenching mechanism of fluorescence of BSA by these

theaflavins, but the dynamic quenching could not be excluded at high concentrations. The binding reaction was spontaneous, and hydrophobic interaction played a major role in the reaction. The banding constants for TF3 and TF2A were significantly higher than those of TF2B and TF1 that lacking the galloyl group on the C-3 position of theaflavins, shown a sequence as TF3 > TF2A > TF2B > TF1, suggesting the importance of the presence of the galloyl moiety on the C-3 position of theaflavins. In addition, the binding ability increased with the increase of molecular weight of quencher. The CD spectra revealed that the change in protein conformation occurred due to the binding of EGCG or TF3 to BSA molecule. Especially, TF3 in high concentration could change the skeleton structure of BSA and induce the unfolding of BSA secondary structure. The present information provides a new perspective for better understanding of the likely physiological fate of these black tea theaflavins.

References

Chen H, Sang S (2014) Biotransformation of tea polyphenols by gut microbiota. J Funct Foods 7:26–42

Clifford MN, Johnston KL, Knight S, Kuhnert N (2003) A hierarchical scheme for LC-MS identification of chlorogenic acid. J Agric Food Chem 51:2900–2911

Del RD, Rodriguez-Mateos A, Spencer JP, Tognolini M, Borges G, Crozier A (2013) Dietary (poly)phenolics in human health: structures, bioavailability, and evidence of protective effects against chronic diseases. Antioxid Redox Signal 18:1818–1892

Greenfield NJ (2006) Using circular dichroism spectra to estimate protein secondary structure. Nat Protoc 1:2876–2890

Kiehne A, Engelhardt UH (1996) Thermospray-LC-MS analysis of various groups of polyphenols in tea. Z Lebensm Unters Forsch 202:48–54

Kroll J, Harshadrai MR, Rohn S (2003) Reactions of plant phenolics with food proteins and enzymes under special consideration of covalent bonds. Food Sci Technol Res 9:205–218

Kuhnert N, Drynan JW, Obuchowicz J, Clifford MN, Witt M (2010) Mass spectrometric characterization of black tea thearubigins leading to an oxidative cascade hypothesis for thearubigin formation. Rapid Commun Mass Spectrom 24:3387–3404

Lakowicz JR (2006) Principles of fluorescence spectroscopy, 3rd edn. Springer, NewYork

Li M, Hagerman AE (2014) Role of the flavan-3-ol and galloyl moieties in the interaction of (−)-epigallocatechin gallate with serum albumin. J Agric Food Chem 62:3768–3775

Li X, Hao Y (2015) Probing the binding of (+)-catechin to bovine serum albumin by isothermal titration calorimetry and spectroscopic techniques. J Mol Struct 1091:109–117

Li D, Zhu M, Xu C, Chen J, Ji B (2011) The effect of Cu^{2+} or Fe^{3+} on the noncovalent binding of rutin with bovine serum albumin by spectroscopic analysis. Spectrochim Acta A 78:74–79

Li S, Lo CY, Pan MH, Lai CS, Ho CT (2013) Black tea: chemical analysis and stability. Food Funct 4:10–18

Li X, Wang G, Chen D, Yan L (2015) β-Carotene and astaxanthin with human and bovine serum albumins. Food Chem 179:213–221

Liu X, Xia W, Jiang Q, Xu Y, Yu P (2015) Binding of a novel bacteriostatic agent—chitosan oligosaccharides–kojic acid graft copolymer to bovine serum albumin: spectroscopic and conformation investigations. Eur Food Res Technol 240:109–118

Menet MC, Sang S, Yang CS, Ho CT, Rosen RT (2004) Analysis of theaflavins and thearubigins from black tea extract by MALDI-TOF mass spectrometry. J Agric Food Chem 52:2455–2461

Ozdal T, Capanoglu E, Altay F (2013) A review on protein–phenolic interactions and associated changes. Food Res Int 51:954–970

Pal S, Saha C, Hossain M, Dey SK, Kumar GS (2012) Influence of galloyl moiety in interaction of epicatechin with bovine serum albumin: a spectroscopic and thermodynamic characterization. PLoS ONE 7:e43321. doi:10.1371/journal.pone.0043321

Pan MH, Lai CS, Wang H, Lo CY, Ho CT, Li S (2013) Black tea in chemo-prevention of cancer and other human diseases. Food Sci Hum Wellness 2:12–21

Papadopoulou A, Green RJ, Frazier RA (2005) Interaction of flavonoids with bovine serum albumin: a fluorescence quenching study. J Agric Food Chem 53:158–163

Rawel HM, Frey SK, Meidtner K, Kroll J, Schweigert FJ (2006) Determining the binding affinities of phenolic compounds to proteins by quenching of the intrinsic tryptophan fluorescence. Mol Nutr Food Res 50:705–713

Roy AS, Tripathy DR, Chatterjee A, Dasgupta S (2013) The influence of common metal ions on the interactions of the isoflavone genistein with bovine serum albumin. Spectrochim Acta A 102:393–402

Simion AM, Aprodu I, Dumitraşcu L, Bahrim GE, Alexe P, Stănciuc N (2015) Exploring the heat-induced structural changes of β-lactoglobulin-linoleic acid complex by fluorescence spectroscopy and molecular modeling techniques. J Food Sci Technol 52:8095–8103

Soares S, Mateus N, Freitas V (2007) Interaction of different polyphenols with bovine serum albumin (BSA) and human salivary alpha-amylase (HSA) by fluorescence quenching. J Agric Food Chem 55:6726–6735

Sreerama N, Woody RW (2000) Estimation of protein secondary structure from circular dichroism spectra: comparison of CONTIN, SELCON, and CDSSTR methods with an expanded reference set. Anal Biochem 287:252–260

Sułkowska A (2002) Interaction of drugs with bovine and human serum albumin. J Mol Struct 614:227–232

Trnková L, Boušová I, Staňková V, Dršata J (2011) Study on the interaction of catechins with human serum albumin using spectroscopic and electrophoretic techniques. J Mol Struct 985:243–250

Wang D, Lu J, Miao A, Xie Z, Yang D (2008a) HPLC-DAD-ESI-MS/MS analysis of polyphenols and purine alkaloids in leaves of 22 tea cultivars in China. J Food Compos Anal 21:361–369

Wang K, Liu Z, Huang JA, Dong X, Song L, Pan Y (2008b) Preparative isolation and purification of theaflavins and catechins by high-speed countercurrent chromatography. J Chromatogr B 867:282–286

Ware WR (1962) Oxygen quenching of fluorescence in solution: an experimental study of the diffusion process. J Phys Chem 66:455–458

Wei YL, Li JQ, Dong C, Shuang SM, Liu DS, Huie CW (2006) Investigation of the association behaviors between biliverdin and bovine serum albumin by fluorescence spectroscopy. Talanta 70:377–382

Xu H, Yao N, Xu H, Wang T, Li G, Li Z (2013) Characterization of the interaction between eupatorin and bovine serum albumin by spectroscopic and molecular modeling methods. Int J Mol Sci 14:14185–14203

Xu D, Wang Q, Zhang W, Bing H, Li Z, Zeng XX, Sun Y (2015) Inhibitory activities of caffeoylquinic acid derivatives from Ilex kudingcha C. J. Tseng on α-glucosidase from Saccharomyces cerevisiae. J Agric Food Chem 63:3694–3703

Zhang G, Wang A, Jiang T, Guo J (2008) Interaction of the irisflorentin with bovine serum albumin: a fluorescence quenching study. J Mol Struct 891:93–97

Zhao H, Ge M, Zhang Z, Wang W, Wu G (2006) Spectroscopic studies on the interaction between riboflavin and albumins. Spectrochim Acta A 65:811–817

Zheng WJ, Wan XC, Bao GH (2015) Brick dark tea: a review of the manufacture, chemical constituents and bioconversion of the major chemical components during fermentation. Phytochem Rev 14:499–523